Indonesian Journal of Physics
Vol. 36. No.1, 30, October, 2025

The Analyse of Barton Pendulum for Application of Resonance Experiment for Senior High School Student

Alfi Nur Albab[1], Berlian Oka Irvianto[1], Nina Siti Aminah[1], Maria Evita[1*]
[1]*Department of Physics, Faculty of Mathematics and Natural Sciences, Jalan Ganesha No. 10, Bandung 40116, Indonesia*

(Received: 2025-08-04, Revised: 2025-11-13, Accepted: 2025-11-19)

Abstract

While pendulums have been around for thousands of years and have even been successfully incorporated into high school curricula, they are still minimally used in Physics experiments on resonance materials. In this study, we designed the Barton Pendulum as a simple laboratory kit operated by teachers and easily observed by students. The pendulum system consists of a series of objects and a small ball connected and suspended with a carbolic string. The small ball here is none other than the trigger that makes all objects oscillate. As an observation material, the length of the string for each object is made different (40 cm, 29.8 cm, 20 cm, 9.5 cm, 6.7 cm). The period of each object in the system is observed using a stopwatch so that the oscillation frequency of each object is known. The object that resonates with the ball is the object that has the same length as the length of the hanging string of the ball, which means that this object has the same natural frequency as the frequency of the ball. The phase difference between the object and the trigger is also observed. The phase difference is equal to $\frac{\pi}{2}$ rad for objects with a string length equal to the length of the trigger string, and the phase difference is equal to π rad for objects with a string length longer than the length of the trigger.

Keywords: Barton pendulum, natural frequency, resonance, phase difference, length of string

INTRODUCTION

A lot of phenomena in everyday life are related to physics, one of which is resonance. In resonance, there is a quantity known as the natural frequency which is the frequency inherent in an object due to the unique elasticity and inertia of the object. If a disturbing force is applied to an object with a disturbance frequency equal to the natural frequency of the object, resonance occurs. The collapse of the Tacoma Bridge in Washington DC is one of the losses caused by resonance. The neglect of the bridge construction details resulted in resonance between the wind vibration and the bridge, which affected the balance of the bridge. Even before the construction of the bridge was completed, a peculiarity could be observed, namely, the ripples flowing along the bridge even in the slightest breeze. The water ripples that appear are water vibrations generated by vibrations from the bridge. The frequency of vibrations exerted continuously by the wind on the bridge has the same value as the natural frequency of the bridge. Even winds that were not very strong (about 40 miles per hour) were strong enough to make the bridge rotate violently so that at 11:00 am on 7 November 1940 the bridge collapsed. The bridge experienced increasingly large oscillations, causing the bridge structure to fail and the bridge to collapse [1].

The collapse of the Nimitz freeway in California in 1989, which necessitated the relocation of the road route in 1997 [2], is a remarkable historical record of freeways. This event is also an example of the negative impact of resonance. The Loma Prieta earthquake that occurred on the San Andreas fault (not on a secondary fault) [3] and followed the 1906 San Francisco earthquake [4] was the beginning of this resonance. The Nimitz freeway, built on the mudflats of Francisco Bay [3], has a natural frequency of about 2.5 Hz [1]. The earthquake frequency corresponds to this natural frequency, which is 0-10 Hz [5]. Resonance

1* Corresponding author. E-mail address: maria@itb.ac.id

occurs so that the subsoil vibrates very strong, resulting in the collapse of the bridge built on it. Other cases affected by resonance include the fields of electricity [6], marine engineering [7], and many other fields.

Wave resonance is very important to learn in order to anticipate the impact it can have. In Indonesia school curriculum, the wave theory is learned at grade XI with rare practical activities [8]. Misconceptions in Physics are often found in high school's learning process along with no correlation-with-daily-life explanation [9]. Moreover, practicum that applies scientific procedures (asking questions, hypothesizing, collecting data, observing, concluding, and communicating the results) encourages the student to explore more about the subject thereby enhancing their curiosity. Curiosity that continues to be nurtured can trigger students' excitement and enthusiasm in learning Physics, which has been considered a difficult and less attractive subject. Therefore, resonance practicum should be given included in the curriculum, as a prerequisite for the next topics such as: standing waves or open and closed organ pipes.

The limited supply of equipment has prevented the practicum of the resonance topic. For example: some surveys about practicum in Physics topics have been conducted to 60 students at SMAN 1 Pabuaran, SMAN 1 Ciomas, and MAN 2 Serang City, resulting in: 25% for fluid, 15% for elasticity, 50% for measurement, and 10% for dynamics topics, while there is no practicum for resonance topic [10]. This is due to the unavailability of resonance practicum tools. Generally, resonance is practiced through a series of sound wave resonance tubes. The phenomenon is not easy to be observed, hence it is not easy to determine the physical quantities [11]. In addition, such an expensive device (frequency oscillator or waveform generator) should also be used for this practicum.

Another lab kit that has been developed is Transverse wave resonance based on Melde's Law. The resonance frequency between the string and the vibration source is used to determine the relationship between the wave propagation speed and the mass of the load, and then the resonance pattern of the fundamental frequency and the higher harmonics is also obtained. However, an additional resonant tube is required for this kit. [12]. In addition, the number of cables complicates the practicum setup for students. However, this kit completes the previous one. Based on the explanation above, it can be seen that the resonance is easier to demonstrate using string as a medium. To overcome the limitation in existing kit, this research proposes a Barton pendulum for the resonance practicum. The advantage of this Barton pendulum kit is the simplicity of the equipment because it does not require electricity and additional devices. The simple practice of resonance through Barton's pendulum can help students in understanding complex systems. Simple pendulums are utilized in complex systems such as pendulum seismometers [13]. The characteristic of a simple pendulum that tends to always stabilized against low-side gravitational potential energy is also often used by engineers to design suitable deformation mechanisms as sensing or control components [14]. Single-wheel pendulum mobile robots have more flexibility than other types of wheeled robots [14] because they are developed based on the concept of simple pendulum control.

EXPERIMENTAL METHOD

Barton's pendulum system consists of a series of objects and a small ball connected by a string (Figure 1). The small ball (trigger, in figure 1) with a mass of 25.31 grams will carry enough potential energy to move the objects through the string ($\pm 1.3\ x\ 10^{-2}$ Joules). Table 1 shows the description about the mass of suspended objects and the length of the string suspending them.

Table 1. The Description of The Objects

Object	Mass of Object (kg)	Length of String (cm)
A	0.00013	40
B	0.000106	29.8
C	0.000059	20
D	0.000083	9.5
E	0.000054	6.7
Trigger	0.000046	20

The lightweight object (Parts A, B, C, D, and E in Figure 1) (mass 2.87 grams) does not require too much gravitational potential energy propagation, following Newton's Second Law that the external force is directly proportional to the mass of the object ($\vec{F} \sim m$). The length of the string hanging the object was varied so that the frequency and phase difference characteristics of the object oscillations could be observed with a string length equal to the length of the trigger string (20 cm, part C of Figure 1), shorter (9.5 cm and 6.7 cm, parts D and E of Figure 1), and longer (40.0 cm and 29.8 cm, parts A and B of Figure 1) than the string length of the small ball. The structure of the system was constructed from ½" Rucika PVC pipes and connected with pipe joints of the same size. For deviation angle variation measure the deviation angle, the kit also includes a Butterfly arc with a precision of 1°. A ½" pipe clamp is attached to the upper horizontal pipe to hook the string through the bolt of the clamp.

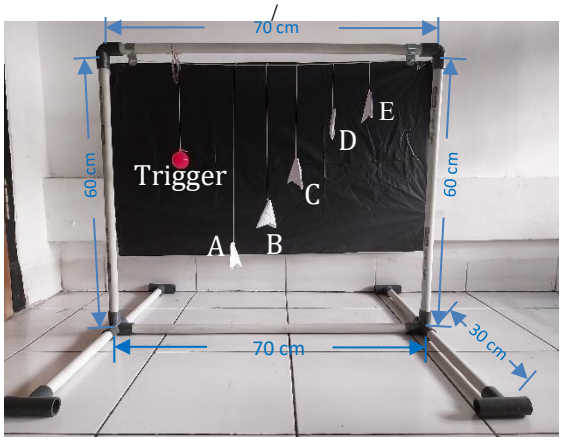

Fig.1. Schematic of the proposed Barton pendulum system.

The data collection begins by first ensuring that the object was in a stationary position. The trigger varied in deviation angles of 30°, 45° and 60° to observe the osilation period. The selection of the angle of deviation aims to facilitate the observation of the oscillation period. In order to obtain a tolerance value for simple harmonic motion, research by [15] revealed that the period formulation used for relatively large angles of deviation uses an infinite series.

Observations were made by looking along the pendulum line and observing the resonance effect arising in each object due to the deviation of the trigger. The period of each object and trigger was measured using a digital stopwatch available on the website www.timeme.com with an accuracy of up to 0.001 s. The experiment was repeated three times for each deviation angle. Each repetition of the minimum of 30 object oscillations to validate the period that had been obtained. The determination of the amplitude point is the most influential parameter in measuring the period of object oscillation. This measurement starts when the object is at the amplitude point and ends when the object returns to the amplitude point. Since the resonance analysis was conducted on the oscillation frequency, the period values obtained were then inverted ($f = \frac{1}{T}$). The oscillation frequencies of all objects were then compared with the trigger oscillation frequencies at all angles of deviation.

RESULTS AND DISCUSSION

Based on the observations made on all objects, it is found that the object with the string length equal to the trigger string length (object C) has the same frequency as the trigger frequency.

The frequency values obtained from the graph should show stability (constant values) for each object at each deviation angle. The frequency trend of object C and the trigger shows the most stable frequency values among all objects, and objects D and E show better frequency stability than objects A and B. The variance in the frequency values of each object is generally caused by the incorrect determination of the amplitude point at certain repetitions of the oscillation. Difficulties were experienced in visual observation of the oscillations of objects A and B due to the small oscillation deviation (amplitude = ±1 cm). Whereas in objects D and E, the short hanging string of the object makes the oscillation of the object often random, not constantly in one trajectory (±3 oscillations out of 10 oscillations of the object are in different oscillation trajectories), or it can be said that at certain times the object oscillates not in simple harmonic motion. The open environment of

the observation site gives the wind a chance to disturb the oscillation of the short string.

The resonance is obtained by calculating the subtraction or error of the trigger frequency and the oscillation frequency of each object. The natural frequency closest to the trigger frequency has the smallest error of all object oscillation errors. Figure 3 (a), (b), and (c) show that the smallest error or subtraction belongs to the oscillation of object C. The average errors of objects A, B, C, D, and E, respectively at 30° trigger deviation are 0.404, 0.191, 0.035, 0.133, and 0.098, respectively. The average errors of objects A, B, C, D, and E, respectively at 45° trigger deviation are 0.393, 0.174, 0.017, 0.067, and 0.036, respectively. The average errors of objects A, B, C, D, and E, respectively at 60° trigger deviation are 0.371, 0.176, 0.005, 0.029, and 0.0293, respectively. Thus, the resonant in this observation is object C. Objects D and E, which have shorter strings than object C's string, oscillate with greater natural frequencies than objects A and B at all trigger deviation angles.

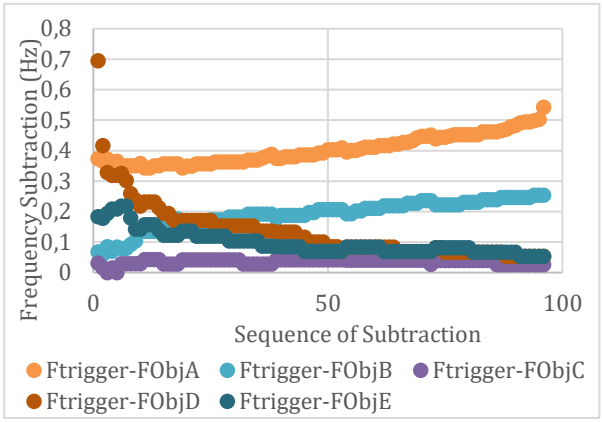

(a)

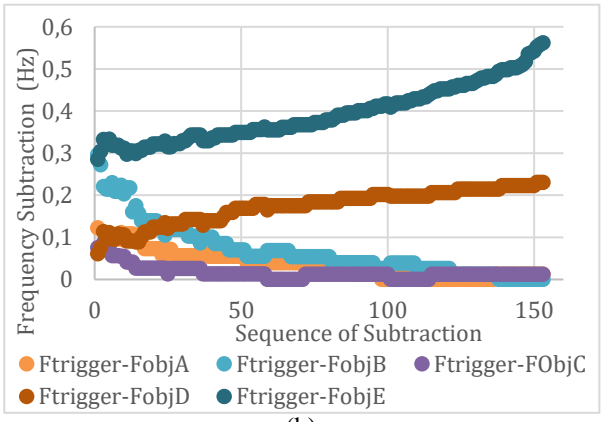

(b)

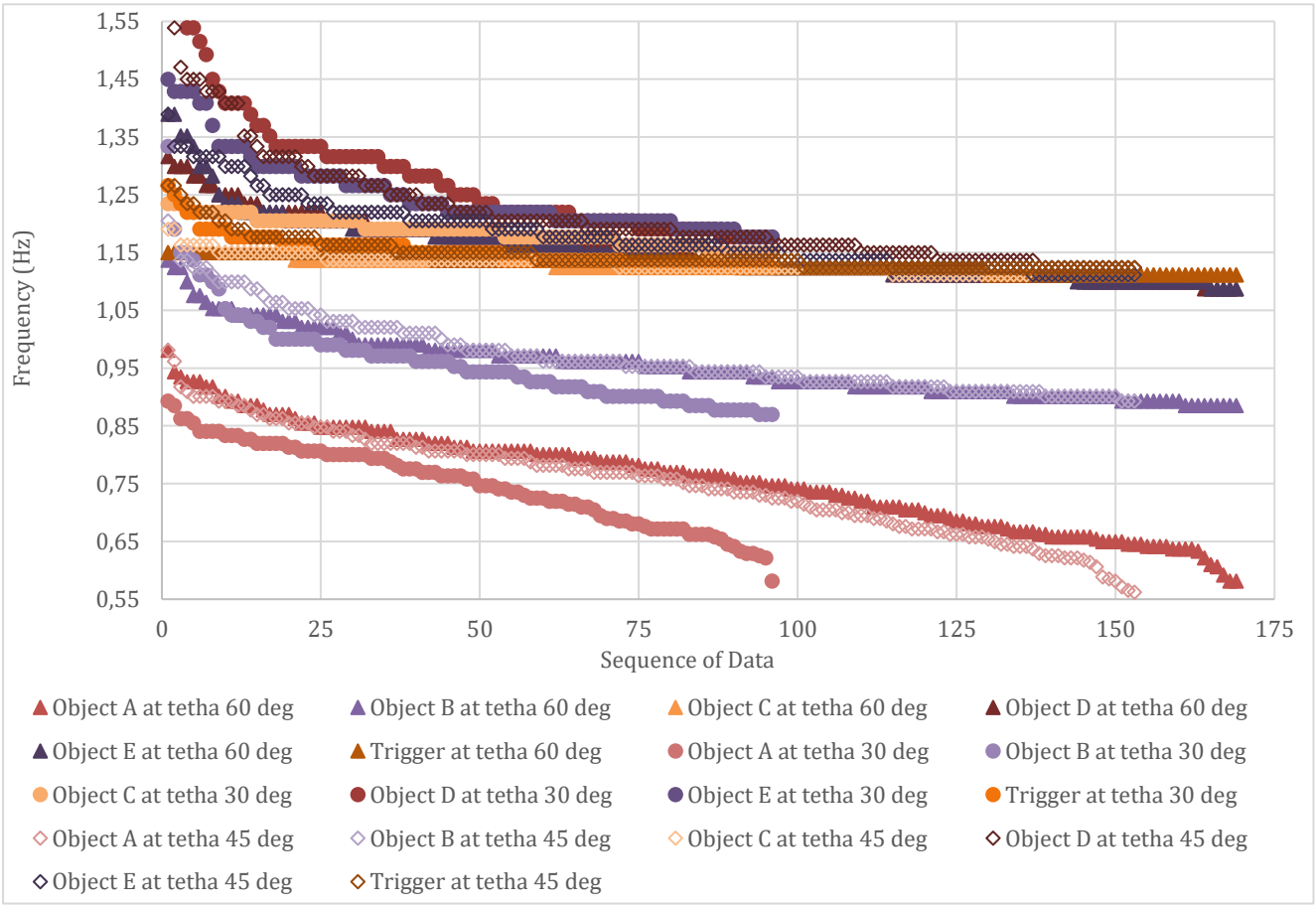

Fig.2. The frequency of the object and the trigger at deviation angle of 30°, 45°, and 60°.

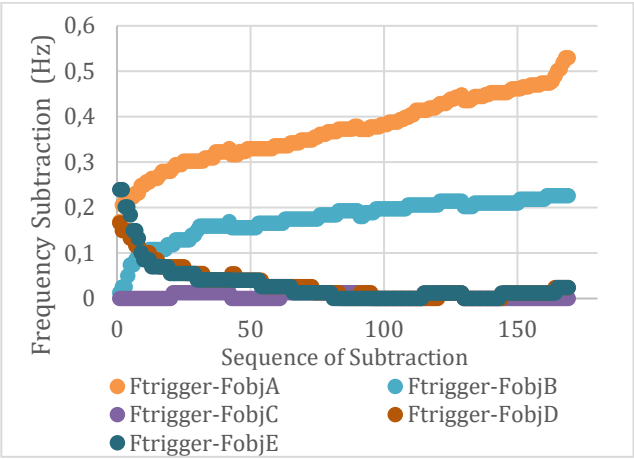

(c)

Fig.3 The Frequency Subtraction of Trigger Frequency to the Other Objects Frequency at deviation Angle of (a) 30°, (b) 45°, and (c) 60°.

Resonance occurs when two objects are synchronised (with the same magnitude) in the same environment [16]. Object C synchronises with the trigger through the frequency magnitude described in the previous paragraph. Each curve in the graph below shows the oscillation frequency corresponding to the amplitude of oscillation. The maximum amplitude extracted from a curve corresponds to the resonant frequency. The resonance curve profile obtained in this study corresponds to the curves obtained in studies by Nayyar in 2015 [17] and Gopal, et al. in 2020 [18].

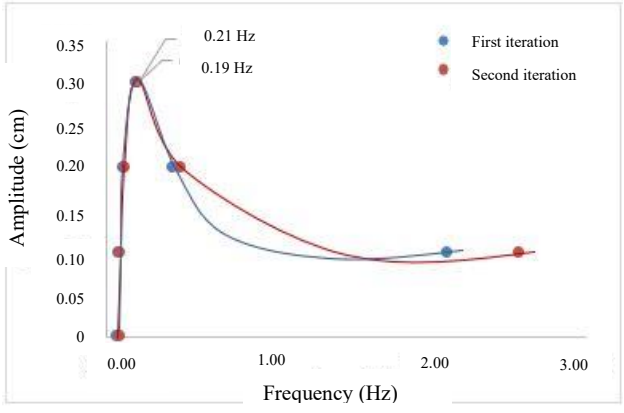

Fig.4. The oscillation frequency of object C (resonant) to the resulted amplitude.

Object C can resonate with the trigger because both have the same string length, this is following the experiments conducted by Anthony Francis-Jones in 2018 [19]. The similarity of frequency due to the similarity of string length can be explained through the analysis of force and angular frequency on the pendulum. When the object swings back and forth with a small angle of deviation, it can be assumed that the object only moves along the x-axis of the circular arc while the motion in the y-axis is ignored [20]. The projection of the string tension force on the x-axis is the restoring force. The period of the pendulum is [20]

$$T = 2\pi\sqrt{\frac{L}{g}} \tag{7}$$

where L is length of the pendulum and g is the constant gravitational acceleration (9.8 m/s^2). From equation (7) above, it can be seen that oscillating objects with the same string length will have the same period and frequency, or it can be said that resonance occurs in two objects that have the same string length in the system. Equation (7) above is valid for θ <10°, otherwise, if the angle of deviation is beyond this limit, then T becomes:

$$T = 2\pi\sqrt{\frac{L}{g}}\left(1 + \frac{1}{2^2}x^2 + \frac{1}{2^2}\frac{3^2}{4^2}x^4 + \cdots\right) \tag{8}$$

where $x = \sin\frac{\theta_m}{2}$ and θ_m is the maximum angular deviation [21]. The first term of equation (8) is for $\theta_m < 10°$, the second term is a correction factor for $\theta_m = 20°$, the third term is a correction factor for $\theta_m = 30°$, and so on. In this research, equation (8) is used to calculate T_{cal} (theoretical oscillation period).

A comparison of T_{cal} and T_{obs} (observed oscillation period) is used to determine the resulting oscillation period by the system.

Table 1. The comparison of T_{cal} and T_{obs}

θ	Object	N (oscillation)	$\overline{T}_{obs}$(s)	T_{cal} (s)	$\lvert\overline{T}_{obs} - T_{cal}\rvert$ (s)
30°	A	96	1.35	1.39	0.04
	B		1.05	1.20	0.15
	C		0.84	0.99	0.15
	D		0.78	0.68	0.1
	E		0.80	0.57	0.23
45°	A	153	1.35	1.49	0.14
	B		1.03	1.29	0.26
	C		0.89	1.06	0.17
	D		0.83	0.73	0.1
	E		0.85	0.61	0.24
60°	A	169	1.33	1.52	0.19
	B		1.05	1.31	0.26
	C		0.89	1.07	0.18
	D		0.87	0.74	0.13
	E		0.87	0.62	0.25

The quantity of θ in Table 1 is the deviation angle of the trigger, N is the number of observed oscillations, $\overline{T}_{obs}$ is the average period in total N oscillations, and $\overline{T}_{cal}$ is the calculated period which is obtained from equation (8). From the table above, the absolute difference between the calculated period and the observed period does not show a significant value, so it can be said that the system has good accuracy.

The oscillation motion of the object cannot be separated from observations about the motion of objects in polar coordinates. The torque of the trigger with mass M is contributed by several forces, so the equation can be written as follows [20]:

$$\vec{\tau}_T = -\mathrm{M}gL\sin\theta \qquad (11)$$

The minus sign shows the direction of the trigger, that is, counterclockwise. $\vec{a}_T$ is the tangential acceleration.

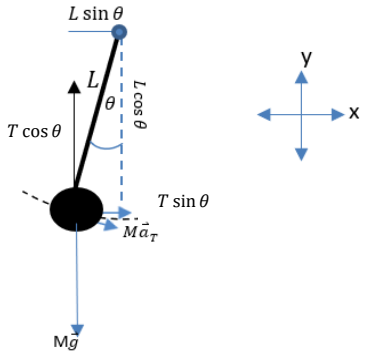

Fig.5. Description of the polar motion of the front-view trigger in 2 dimensions. $M\vec{a}$ is perpendicular to L and $T\sin\theta$ is perpendicular to $T\cos\theta$.

Torque of the resonant having mass m is [20]:

$$\vec{\tau}_R = -mgL\sin\theta \qquad (13)$$

The equation (15) is also applicable for other objects. From equations (12) and (13), it can be seen that the trigger torque is greater than the resonant torque and the torque of other objects. This is due to the mass of the trigger (M) in equation (12) has a value greater than the mass of the object (m) in equation (15), M = 25.31 grams and m = 2.87 grams. The large torque of the trigger causes it to have the largest oscillation amplitude in the system (13 cm).

After the trigger, the object that has a large amplitude is resonant at 0.3 cm. This happens because when the trigger is given a force to swing, the object that has the same natural frequency as the trigger frequency will absorb the best energy transfer ($\pm$4.2 x 10^{-3} J) [23]. This can be viewed from the conservation of energy that applies to the system. The deviation given to the trigger produces maximum potential energy, which is $\pm$3 x10^{-1}J. When the trigger is at the lowest point, then all the potential energy is converted into kinetic energy. The change of potential energy into kinetic energy in the trigger swing is shown by the following equation.

$$\Delta EK = mg\Delta h = \frac{1}{2}(m(\Delta\vec{v})^2) \qquad (14)$$

As the string is assumed to be massless and unstretchable, the string exists only as the connection between two entities [20]. In our system, the connection is between trigger and object A, object B and the resonant, the resonant and object D, as well as object D and

object E. The string pulls on both entities in each connection with the same force magnitude $\vec{T}$ [20]. Thus, we infer that the maximum kinetic energy owned by trigger as shown in equation (14) is not only used by the trigger itself to oscillate again, but also is distributed to all objects through the string. This kinetic energy distribution is not equal among each connection, due to the varying length of the string between objects. The most kinetic energy is received by the resonant, judging from the largest resonant amplitude among all objects (0.3 cm). The length of the string is related to the moment of inertia which is proportional to the torque, as shown by the following equation [20]:

$$\tau_R = I\alpha = \alpha \sum m_i {r_i}^2 \qquad (15)$$

Where α is the angular acceleration and r is the distance between one particle of the object and the axis of rotation. In continuous bodies such as the trigger and the object, r is indicated by L in Figure 5. The trigger and the resonator have the same string length. The previous equation shows the mass distribution of all the constituent particles of the object to the pivot point [23]. The magnitude of the moment of inertia on each object is:

$$I = I_s + I_o = \frac{1}{3} m_s L^2 + m_o d^2 \qquad (16)$$

Where I_s is the moment of inertia of the string with the shaft at the end of the string [23], I_o is the moment of inertia of the object (as well as the inertia moment of trigger), m_s and L are the mass and length of the string when mounted, m_o is the mass of object (as well the mass of trigger), and d is the distance between the object and the shaft. Since the object is attached to the end of the string (Figure 5), L = d. The calculation of the moment of inertia results in 4.70 x 10^{-4} kgm^2; 2.60 x 10^{-4} kgm^2; 1.20 x 10^{-4} kgm^2; 2.60 x 10^{-5} kgm^2; 1.30 x 10^{-5} kgm^2; and 1.01 x 10^{-2} kgm^2 for objects A, B, C, D, E, and the trigger, respectively. Each mechanical system has a certain amount of elasticity and inertia, and consequently has a unique natural frequency [24]. With the same string length, the mass distribution of the resonant string is most nearly the same as the mass distribution of the trigger string. It is this particle mass that carries the kinetic energy so that the resonant gets the largest kinetic energy distribution among all objects and has the same natural frequency as the trigger frequency (f = 1. 15 Hz), as our result of observation shown by figure 2.

The objects oscillate with varying phase differences. In the observations made, it is known that the resonant has a phase difference of ¼ wave (π/2 rad) with respect to the trigger and objects A and B have a phase difference of ½ wave or π rad (Figure 6). Objects that have a shorter string length than the resonant string (objects D and E) were not easily observed in this observation. However, the Harvard Natural Science Lecture Demonstration on copyright 2024 [19] mentions that objects with a shorter string than the resonant string have a phase difference = 0 or in phase with the trigger. The phase difference found in the study indicates the time delay of the kinetic energy distributed on different objects and string lengths [25]. The solution of the phase equation of the trigger and resonant is shown by the following equation [25]:

$$\theta_1 = \frac{\theta_0}{2}\cos(\omega_0 t) + \frac{\theta_0}{2}\cos(\omega' t) \qquad (17)$$

$$= \theta_0 \cos\left(\frac{\omega_0 + \omega'}{2} t\right) \cos\left(\frac{\omega_0 - \omega'}{2} t\right)$$

$$\theta_2 = \frac{\theta_0}{2}\cos(\omega_0 t) - \frac{\theta_0}{2}\cos(\omega' t)$$

$$= \theta_0 \sin\left(\frac{\omega_0 + \omega'}{2} t\right) \sin\left(\frac{\omega' - \omega_0}{2} t\right)$$

The above solution has two frequencies (known as the eigenfrequencies of the system). θ_1 is the phase of the resonant and θ_2 is the phase of the trigger. As expressed mathematically through the above equations, the trigger oscillation is a function of sin and the resonant oscillation is a function of cos (there is a phase difference of π/2 rad). This phase difference indicates the transfer of energy between the trigger and resonant to each other [25].

The research results that have been designed can be used to reflect resonance events that have occurred in nature. Similar to the collapse of the Tacoma Bridge, the Nimitz freeway, etc., resonances that are initially stationary can then oscillate with increasing amplitude when the trigger applies a disturbing force.

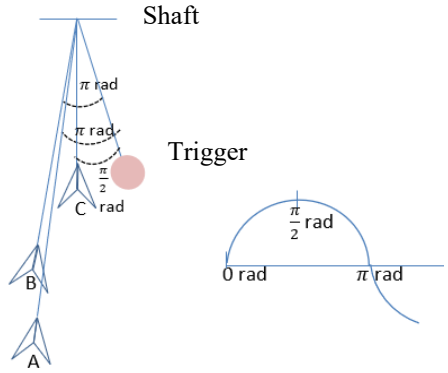

(a) (b)

Fig. 6. (a) The schematic of phase difference of object A, B, and C motion to the trigger, corresponding to simple harmonic motion (b).

Furthermore, from the deviation of object C as a resonant, it can be seen that the resonant is oscillating with a maximum deviation of 0.3 cm (Figure 8). To measure this deviation, a ruler with a smallest scale of 0.1 cm is used so that the deviation can still be observed. Initially, object C oscillates until it reaches an amplitude in the opposite direction (positive-negative direction on the graph). The deviation of the object increases gradually with a maximum amplitude of 0.3 cm and a minimum amplitude of 0.1 cm. Then the velocity of the object decreases (≈0 m/s) until it reaches zero deviation. Then, the object oscillates again with an amplitude range equal to or smaller than the amplitude of the previous oscillation series. The response of the object repeats until it forms a regular behaviour. The existence of damping in the oscillation, which is shown by the decreasing deviation, is assumed to be due to the frictional force of air [26]. The friction force between the damped pendulum and the medium is usually assumed to be directly proportional to the pendulum speed [27]. In this study, the resonant oscillates with a fairly short period (<1 second), which means that the linear and angular velocities of the resonant are large enough and the air friction force is also large enough that the resonant is easily damped. The amplitude of the resonant oscillation continuously decreases as mechanical energy is transmitted to the environment due to the air friction force [28]. The magnitude of this force is proportional to the square of the oscillation speed (for oscillations less than the speed of sound in air) [29].

$$F = \frac{1}{2} C_D \rho A v^2 \qquad (18)$$

where ρ is the air density, v is the resonant linear speed, C_D is the air drag coefficient, and A is the frontal cross-sectional area of the resonant parallel to the resonant direction of motion. Experiments using a 1.5 m high glass tube with an inner radius of 5 cm showed that the unitless value of C_D depends on the shape of the object and the Reynolds number [30].

Pirooz and Shankar (2017) found that although the string has a small or negligible effect in some cases, in general, the string in the pendulum system has a large contribution and in some cases even a greater effect than the damping effect of the object.

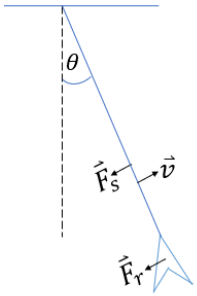

Fig. 7. The detailed air friction force of string $(\vec{F}_s)$ and of the resonant $(\vec{F}_r)$.

$\vec{F}_r$ is the multiplication of linear velocity $(\vec{v})$ by a constant [28].

$$\overrightarrow{F_r} = -c\vec{v}$$

c is an independent constant of linear velocity, but is dependent on the shape and cross-sectional area of an object.

After stopping for a while, the resonant oscillation back due to the disruptive force

given by the trigger continuously. The resonant motion will completely stop as the force stops. Ideally, no outside disruptive forces are acting on the resonator other than the force from the trigger, so that the system is completely closed (free from wind or other sources of disturbance).

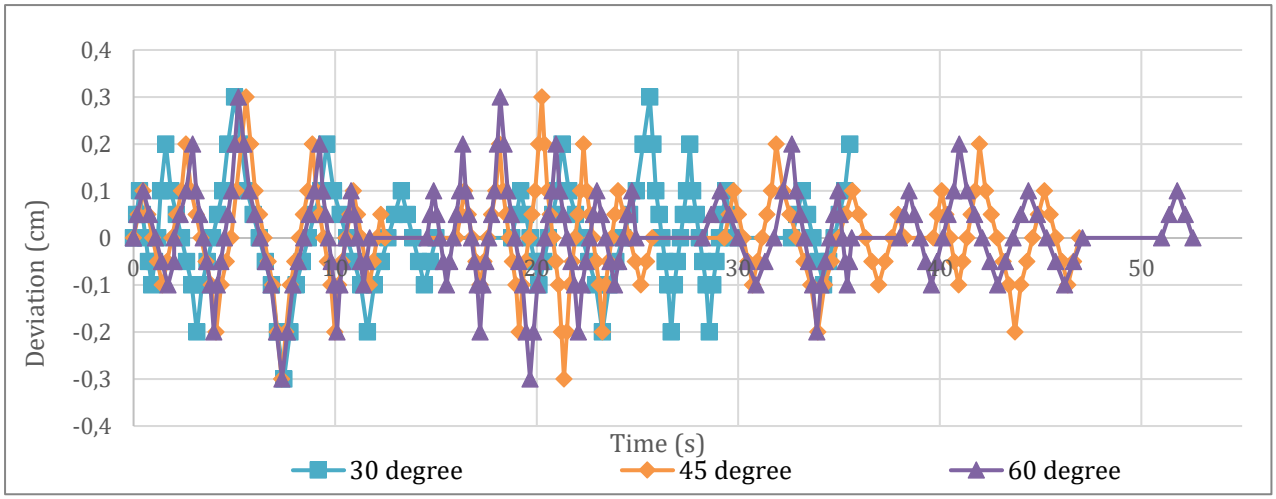

Fig. 8. The deviation of resonant oscillation (Object C).

CONCLUSIONS

Based on our experiment result, we can notice that this practicum kit can be used by senior high school student easily to observe resonance with simple steps and certainly with low production cost. This kit is able to show the resonance phenomenon on the string wave along with the amplitude and phase difference of the object. The object that resonates with the trigger is an object that has a string length equal to the length of the trigger string, namely object C with the length of the hanging string = 20 cm. This is in accordance with the formulation of the relationship between period and string length that has been explained. Of all the objects observed in the system, the object that has the largest oscillation amplitude is the trigger, which is 13 cm, due to the trigger having the largest torque. The next largest amplitude is the oscillation amplitude of the resonator (maximum amplitude = 0.3 cm). The resonator absorbs the energy transfer from the trigger best ($\pm 4.2\ x\ 10^{-3}$)J). The moments of inertia of all objects for objects A, B, C, D, E and the trigger are 4.70 x 10^{-4} kgm^2; 2.60 x 10^{-4} kgm^2; 1.20 x 10^{-4} kgm^2; 2.60 x 10^{-5} kgm^2; 1.30 x 10^{-5} kgm^2; and 1.01 x 10^{-2} kgm^2, respectively. There is a phase difference between the oscillations of the object caused by the travel time of the kinetic energy distribution from the trigger to the object. The $\pi/2$ rad phase difference belongs to resonant, π rad phase difference belongs to objects A and B which have longer string lengths than object C's string length (40 cm and 29.8 cm for objects A and B, respectively), while the phase difference of objects D and E in this study is difficult to observe due to the very fast motion of the objects because they have the shortest hanging strings among all objects (9.5 cm and 6.7 cm for objects D and E, respectively).

ACKNOWLEDGMENT

We would like to say thank you to the Faculty of Mathematics and Natural Sciences of ITB for the PPMI research funds.

REFERENCES

[1] Mikrajuddin, A. Fisika Dasar 1. pp 243. 2016.

[2] Joe, W., Route Change on The American Freeway System, Journ. of Tras. Geo., **67**, pp. 12-23, 2018.

[3] Ping, T., Dinghui, Y., Dongzhuo, L., dan Qinya, L., Time-evolving seismic tomography: The method andits application to the 1989 Loma Prieta and 2014 South Napa earthquake area,

California, Geophys. Res. Lett., **44**, pp. 3165-3175, 2017.

[4] Nims, D., K., Miranda, E., Aiken, I., D., Whittaker, A., S., and Bertero, V., V., Collapse of The Cypress Street Viaduct as A Result of The Loma Prieta Earthquake, 1989.

[5] Hough S. E., Friberg, P. A., Busby, R., Field E. F., Jacob K. H., dan Borcherdt, R. D., Sediment-Induced Amplification and The Collapse os The Nimitz Freeway, Nature, **344**, pp. 853-855. 1990.

[6] Mukhtorhon, I., Ananlysis of Auto Parametric Oscillations at the Subharmonic Frequency in Two-Phase Ferro Resonance Circuits, Proc. of The 11th Intern. Confer. On Appl. Innov. In IT, pp. 285-290, 2023.

[7] Jishnu, K. K., Xiong, L., Jose, M., Chandana, J. G., and Amit, K. G., Mitigation of Resonance Vibration Effects in Marine Propulsion, IEEE Transac. on Indust. Electron., **66** (8), pp. 6159-6169, 2019.

[8]Cindy, M, Efektivitas Model POGIL (Process Oriented Guided Inquiry Learning) Berbantukan Media Praktikum Berbasis Aplikasi Smartphone terhadap Kemampuan Berpikir Kritis Siswa SMA, Skripsi, Fakultas Keguruan dan Ilmu Pendidikan, Universitas Lampung, 2023.

[9] Yuninasurtiana, Pengembangan Model Real-Virtual Conceptual Change Laboratory (R-V CCLab) beserta Perangkatnya untuk Meremediasi Miskonsepsi Peserta Didik SMA terkait Konsep-konsep Fisika, Disertasi, Program Studi Pendidikan Ilmu Pengetahuan Alam, Universitas Pendidikan Indonesia, 2021.

[10] Oriza, N., Alat Praktikum Resonansi Gelombang Bunyi Berbasis Arduino untuk Meningkatkan Keterampilan Proses Sains /Siswa di SMA, Tesis, Universitas Negeri Jakarta, Jakarta, 2020.

[11] Nursulistiyo, E., Design and Development of Multipurpose Kundt's Tube as Physics Leraning Media, International Conference on Mathematics, Science and Education, 2017.

[12] Fatakh, L., P., dan Imam, S., Pengembangan Media Hukum Melde Berbasis Aplikasi Physics Toolbox Sensor Suite pada Materi Gelombang Stasioner, Jur. Inov. Pend. Fis., **7**(2), pp. 165-170, 2018.

[13] Michael, M. and Nicholas, A. B., A swing of Beauty: Pendulums, Fluids, Forces, and Computers. Fluids, **5**, pp1-35, 2020.

[14] Mario E. H., Manuel A., Marco C., and Esther L., Cosimulation and Control of Single-Wheel Pendulum Mobile Robot, Jour. of Mechan. and Robot., **13**, pp. 1-9, 2021.

[15] Yuli, Y., Neng, N. M., dan Dandan, L. S., Pengaruh Panjang Tali, Massa, dan Diameter terhadap Periode dengan Variasi Sudut Simpangan, Jurn. STRING, **5** (1), pp. 6-10, 2020.

[16] Jin, W., Qilong, X., Lixin, L., Baolin, L., Leilei, H., and Yang, C., Dynamic Analysis of Simple Pendulum Model under Variable Damping. Alexandr. Engin. Jour., **61**(12), pp. 10563-10575, 2022.

[17]Abhishek, N., Power Generation using Lock-in Vortex Shedding Frequencies from Quasi-constant Airflow, Thesis, Departement of Mechanical Automotive and Materials Engineering, University of Windsor, 2015.

[18] Gopal, R., Chilaka, V. K., Sangay, T., and Parsu, R. S., Development of Experimental Equipment to Study Mechanical Resonance, Annual College Research Grant Report, pp. 1-19, 2020.

[19] Barton's Pendulum, https://sciencedemonstrations.fas.harvard.edu/presentations/bartons-pendulum (accessed at July 23th 2024)

[20] Halliday dan Resnick, Fundamental of Physics, 10th ed, Wiley, 2014.

[21] Ganijanti, A. S., Seri Fisika Dasar Mekanika, Salemba Teknika, pp 185, 2002.

[22] Jerome, D., and Muneo, K., The Concept of Resonanc[e: From Physics to Cognitive Psychology. Cognitive 2020: The Twelfth International Conference on Advanced

Cognitive Technologies and Applications. pp. 62-67, 2020.

[23] Alan G., Betty M., R., dan Robert C. R., Physics, McGraw-Hill, 2010.pp 263-264.

[24] F-J's Physics-Barton's Pendulum and Resonance-Video 35, https://www.youtube.com/watch?v=W4YaemEauGo (accessed at July 23th 2024)

[25] Timon, I., Mechanics and Relativity, pp. 89, 2018.

[26] Defrianto, P., Modelling Large-Angle Pendulum Oscillations with Quadratic Damping and Damping on The String, Jurn. Pend. Fis., **10** (2), pp. 101-106, 2022.

[27] Quiroga, G. D. dan Ospina-Henao, P., A., Dynamics of Damped Oscillations: Physical Pendulum, Eur. J. Phys., **38**(6), 2017.

[28] Mohazzabi, P. dan Shankar, S. P., Damping as A Simple Pendulum Due to Drag on Its String. Jour. Of Appl. Math. And Phys., **5**(1), 2017.

[29] Mohazzabi, P. dan Fields, J.C., High-Altitude Projectile Motion. Canadian Journal of Physics, **82**, pp. 197-204, 2004.

[30] Dioguardi, F., Mele, D., dan Dellino, P., A New One-Equation Model of Fluid Drag for Irregularly Shaped Particles Valid over A Wide Range of Reynoalds Number, Journ. Of Geophys. Res., **123** (1), pp. 144-156, 2017.